

SANDIA REPORT

SAND2003-8198
Unlimited Release
Printed April 2003

The Dormancy phase in LIGA micro-gears

S. Aubry, R. E. Jones, J. A. Zimmerman

Prepared by
Sandia National Laboratories
Albuquerque, New Mexico 87185 and Livermore, California 94550

Sandia is a multiprogram laboratory operated by Sandia Corporation,
a Lockheed Martin Company, for the United States Department of Energy's
National Nuclear Security Administration under Contract DE-AC04-94AL85000.

Approved for public release; further dissemination unlimited.



Sandia National Laboratories

Issued by Sandia National Laboratories, operated for the United States Department of Energy by Sandia Corporation.

NOTICE: This report was prepared as an account of work sponsored by an agency of the United States Government. Neither the United States Government, nor any agency thereof, nor any of their employees, nor any of their contractors, subcontractors, or their employees, make any warranty, express or implied, or assume any legal liability or responsibility for the accuracy, completeness, or usefulness of any information, apparatus, product, or process disclosed, or represent that its use would not infringe privately owned rights. Reference herein to any specific commercial product, process, or service by trade name, trademark, manufacturer, or otherwise, does not necessarily constitute or imply its endorsement, recommendation, or favoring by the United States Government, any agency thereof, or any of their contractors or subcontractors. The views and opinions expressed herein do not necessarily state or reflect those of the United States Government, any agency thereof, or any of their contractors.

Printed in the United States of America. This report has been reproduced directly from the best available copy.

Available to DOE and DOE contractors from
U.S. Department of Energy
Office of Scientific and Technical Information
P.O. Box 62
Oak Ridge, TN 37831

Telephone: (865)576-8401
Facsimile: (865)576-5728
E-Mail: reports@adonis.osti.gov
Online ordering: <http://www.doe.gov/bridge>

Available to the public from
U.S. Department of Commerce
National Technical Information Service
5285 Port Royal Rd
Springfield, VA 22161

Telephone: (800)553-6847
Facsimile: (703)605-6900
E-Mail: orders@ntis.fedworld.gov
Online order: <http://www.ntis.gov/help/ordermethods.asp?loc=7-4-0#online>



SAND2003-8198
Unlimited Release
Printed April 2003

The Dormancy phase in LIGA micro-gears

Sylvie Aubry ¹,
Reese E. Jones, ²
and Jonathan A. Zimmerman ³

Science-based Materials Modeling Department 8726
Sandia National Laboratories
P.O. Box 969
Livermore, CA 94551

¹Sylvie Aubry (saubry@sandia.gov)

²Reese E. Jones (rjones@sandia.gov)

³Jonathan A. Zimmerman (jzimmer@sandia.gov)

This page intentionally left blank.

Abstract

Sandia National Laboratories are interested in obtaining a thorough understanding of how aging processes affect the reliability and performance of weapon components. Microscale parts that are manufactured using the LIGA process are being considered as replacements in the refurbished weapons and life extension programs. Dormancy issues are particularly relevant to these parts.

In this report, a method to study the dormancy phase and adhesion force of two nickel LIGA micro-gears in contact is presented. It is based on an analysis of the preferred states of the system, which correspond to local energy minima. The system is inactive for a long period of time and the assumption is made that, from a microscopic point of view, it reaches an equilibrium state that corresponds to a local, if not global, energy minimum. Energy minima do not correspond exactly to states of equilibrium in the system but are important states since they have higher probabilities to be present after dormancy than other states. The configuration with the highest probability corresponds to the global energy minimum.

This report considers a system composed of two micro-gears in contact for a long period of time in a special storage environment. The questions arising in this problem are: first what will the interface of the two micro-gears look like after the dormancy period, and, second what will be the force necessary to pull both micro-gears apart or equivalently what is the adhesion force at the interface of the surface of the gears?

In this particular system, details of the microstructure are of the order of the nanometer and so are sufficiently small to be analyzed at the atomic scale. Thus, particle simulation techniques are explored to analyze the evolution of these details with time. The system which is studied in this report is a mathematical simplification of the real system. The goal is to understand how the shape of the asperity influences its behavior. The asperities were placed in contact in various combinations and a study of how the shape and the offset of two asperities in contact influence their behavior is done in this report. The dormancy phase is modeled by looking at energy minima of the system and is implemented using molecular static simulations. Also the adhesion force is estimated using molecular dynamics and the evolution of the force necessary to pull the two asperities in contact apart is evaluated for different possible shapes and dimensions.

Keywords:

Dormancy Phase, aging, diffusion, corrosion, adhesion, creep, atomistic, molecular dynamics, molecular statics, energy minimization, Monte Carlo.

This page intentionally left blank.

Contents

1	Introduction	9
2	Statement of the Problem	13
2.1	Experimental background	13
2.2	Description of the mechanisms	16
2.2.1	Adhesion	16
2.2.2	Creep	17
2.2.3	Oxidation	17
2.2.4	Diffusion	18
2.3	Relations between mechanisms	18
2.4	External Conditions	18
3	Simulation Methods	21
3.1	Equilibrium and Energy Minimization	21
3.2	Implementation of atomistic simulation methods	22
3.2.1	Molecular dynamics	22
3.2.2	Energy minimization techniques	24
3.3	Description of the numerical model	25
3.3.1	Details of implementation: boundary conditions	25
3.3.2	Specific details of the system	26
4	Simulation of aging and adhesion forces	29
4.1	Numerical simulation of aging via energy minimization	29
4.2	Numerical simulation of adhesion	34
4.3	Study of a simulated system with dimensions of a physical system	35
5	Conclusion	45
6	Future Work	47
7	Bibliography	49
7.1	Distribution	52

List of Figures

2.1	AFM figures of LIGA Micro-Gears. Images taken from S. Prasad, A. Hall and M. Dugger [Prasad et al., 2000]. Note the regular columnar microstructure of the top sidewall's tooth.	14
2.2	Surface roughness and position of asperities	15
2.3	Mechanisms involved in the interaction of two surfaces with time. Diffusion influences all areas.	16
3.1	Description of the studied system	26
3.2	Definition of the radius R and boundary conditions. The asperity is shown in red.	26
4.1	Relaxation of a simple bump of nickel	29
4.2	Initial and final state of the atoms after aging	31
4.3	Initial and final state of the atoms after aging	32
4.4	Initial and final state of the atoms after aging	33
4.5	Snapshots of MD simulation of pulled-apart force	37
4.6	Reaction force on top and Energy per atom on the bottom for an offset of $1/2$. Note that for this range of rates, the curves overlap.	38
4.7	Reaction force on top and Energy per atom on the bottom for an offset of $1/2$. Note that for this range of rates, the curves do not overlap.	39
4.8	Reaction force for special offsets at $7\text{\AA}/ms$	40
4.9	Final state of the atoms after aging for a physical dimension problem	41
4.10	Close-up of the final state of the atoms after aging for a physical dimension problem	42
4.11	Close-up of the final state of the atoms after molecular dynamics simulation for a physical dimension problem after separation	43
4.12	Reaction force on top and Energy per atom on the bottom for an offset of $1/2$ for a physical dimension problem	44

Chapter 1

Introduction

Sandia National Laboratories are actively engaged in an important effort to develop and fabricate high aspect ratio micro-machines for a variety of applications. One such effort is the development of LIGA technology. Basically, LIGA is a micro machining technology originated in the early 1980s, [LIGA, 2001]. As originally implemented, highly parallel x-rays from a synchrotron are incident on a mask patterned with high Z absorbers. The absorbers on the mask are thick enough to prevent the penetration of x-rays. In the open areas of the mask, the radiation passes through and exposes PMMA (polymethylmethacrylate) resist. The resist is then developed and the resulting PMMA mold is used to produce a metal part by electroplating in the developed regions. The electroplating is either the final step in the process or the electroplated part is used as a mold for replication from another material such as plastic or ceramic. By using the penetrating power of x-rays from a synchrotron, LIGA allows the fabrication of structures which have vertical dimensions from hundreds of microns to millimeters and horizontal dimensions which can be as small as microns. These are 3-D microstructures defined by 2-D lithographic patterns. The height-to-width ratio capability is relevant to the manufacturing of miniature components that can withstand high pressure and temperature, and can transfer useful forces or torques. The material flexibility also offers opportunities to fabricate miniature components using LIGA instead of precision machining approaches such as wire EDM. The feature definition, radius, and side wall texture using LIGA are superior to current precision machining techniques.

These micro-machines are being considered as replacement parts of weapons components, and reliability of performance must be ensured before their incorporation into bigger systems. The dimensions of these devices are sufficiently small that their mechanical behavior differs from macro-scale parts. Phenomena such as adhesion and friction do not operate in the usual manner at smaller scales. Several micro-systems have been constructed and studied, see for example [Brück et al., 2000], [Tanner et al., 2000], and dormancy issues related to size and microstructure have started to gain interest. Several micro-systems have been studied and built already, examples include: millimotor, precision stepping motor rotors and stators, mass spectrometer, heat exchanger etc.

Optimization of the properties of LIGA micro-parts is still under development, as is an understanding of how process parameters affect the characteristics of shape, microstructure and mate-

rials composition. The fabrication process gives the surface its nature. The exact composition of the nature of the surface influences the behavior of the final gears and changes their macroscopic properties. Also since macroscopic properties are strongly dependent on its microstructure, any change in the microstructure will influence the yield stress and material anisotropy. The analysis of aging in parts that are still evolving is not an easy task but some experimental set-ups have been employed using currently constructed parts [Yang and Kelly, 2002].

An effort of Sandia National Laboratories in modeling the aging of micro-systems exists both at the experimental and numerical levels. A common experimental method used to simulate aging is to increase the temperature of the system and to measure the evolution of the strength of the parts with increasing temperature. The evolution of mechanisms such as adhesion, static friction, internal fracture etc. can then be monitored through test failure analysis and performance of the part under study can then be better understood. The idea is to find laws which dictate these phenomena with time. This method, called accelerated aging or annealing has shown that the strength of LIGA parts decreases with increasing temperature.

Drawbacks of this method are that it does not give a clear picture of what is really related to aging and what is related to the effect of excessive temperature and it is not sufficient to get an idea of performance and reliability of LIGA micro-parts. Other complementary studies are then made such as developing numerical models to study the grain boundary sliding via atomistic and first principles calculations [Hamilton, 2001] or to study evolution of the microstructure by building an finite element mesh based on AFM data [Redmond et al., 2001] etc. Some molecular dynamics simulations have also been made to understand how certain basic mechanisms behave at the molecular time scale (in the order of the nano-second) [Chandross et al., 2003].

Methods to study performance and reliability of micro-parts are numerous at Sandia [Hamilton, 2001], [Tanner et al., 2000], [DeBoer and Mayer, 2001] and [Dugger, 2002]. Another method to study aging is to make direct measurements of degradation of a system left alone for a certain period of time. N. Yang and co-workers [Yang and Kelly, 2002] have been doing experiments on the behavior of LIGA gears submitted to temperature cycle where the temperature does not exceed a third of the melting point of nickel. Their experiment consists of monitoring the evolution of the microstructure of nickel LIGA micro-gears with time which are either pinned alone or pinned and held in contact with springs in a special nitrogen storage environment. Data on the evolution of the microstructure and the development of an interface between two gears in contact have been collected and are in the process of being analyzed. This will help our understanding of the degradation of these parts. These experiments will have a big impact on the reliability of constructed parts and will reveal possible defects linked to the fabrication process. They will also be a good source of data for validation of numerical models.

In this report, we present an analytical and numerical method to determine how a system constituted of two micro-gears in contact evolves with time and if it will function properly after being left in contact for a long period of time. Since the macroscopic time scale is out of range for direct simulation, we consider that the state in which the system will be after a long period of time corresponds to one of its local minima of energy. These special energy states have a favorable probability to be present. The adhesion force between gears, which could prevent the system from working properly can be computed when the system is in one of its local minima. This gives an

estimate of the force necessary to pull the two micro-gears apart after they have been lying dormant for a long period of time.

More precisely, we first study local minima of a system consisting of two asperities in contact and then we compute the force necessary to pull them apart. Different shapes and dimensions of asperities are considered corresponding to actual reported sizes and we show how these parameters influence the results.

We start by recalling experimental results of Prasad *et al.* [Prasad et al., 2000] regarding nickel LIGA micro-gears surface structure which is at the root of our analysis, then we identify the main mechanisms acting on the system in chapter 2. We review existing atomistic methods, and we show how they can be applied to the problem under consideration in chapter 3. Finally we present numerical results which emphasize specific properties of LIGA parts left in contact for a long period of time. These properties include the local minima, energy and force necessary to break the interface constructed with time in chapter 4. This report provides preliminary results which will be used as a precursor when we use a global energy minimization method to study aging of the micro-gears system.

This page intentionally left blank.

Chapter 2

Statement of the Problem

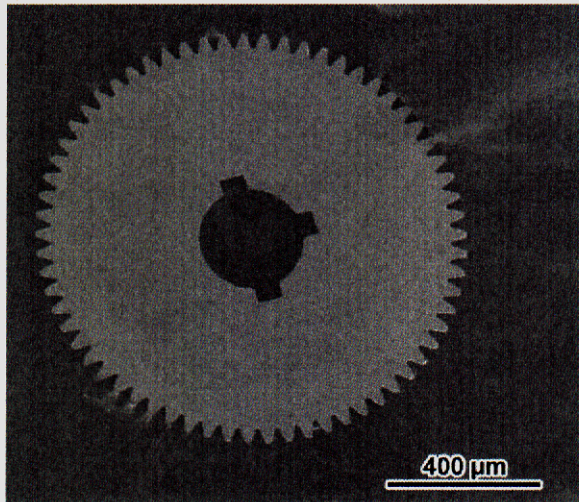
Several investigations of the microstructure and mechanical properties of LIGA micro-gears have been done [Prasad et al., 2000], [Yang and Kelly, 2002]. Characteristics of the surface such as roughness, shape of the asperities etc. are essential in this work. Their sufficiently small dimensions allow a study at the atomic level. This is not the case, for example, for the micro-machines fabricated in silicon at Sandia National Laboratory, NM where a typical size of the details of the microstructure such as asperities is several orders of magnitude higher than nickel LIGA, and is too large for atomistic studies [DeBoer et al., 1999], [DeBoer et al., 2000], [Redmond et al., 2001]. Other methods can be introduced to study this microstructure, such as the continuum model of Greenwood-Williamson [Greenwood and Williamson, 1966] using the finite element method [Redmond et al., 2001].

2.1 Experimental background

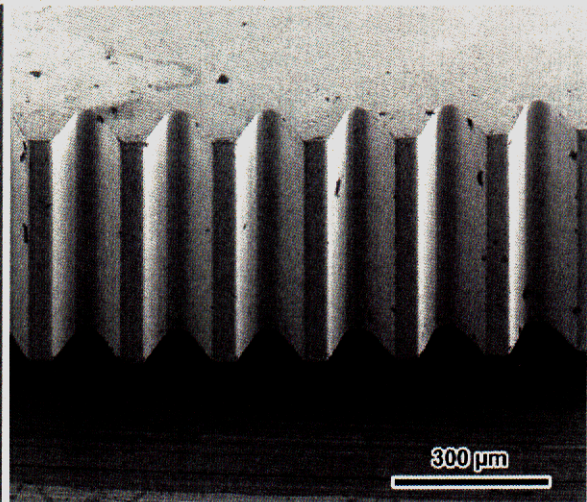
Prasad *et al.* [Prasad et al., 2000] have studied the nature of the surface of LIGA micro-gears as well as the way they interact with each other during sliding contact. They quantified the surface roughness using atomic force microscopy (AFM) and showed that the sidewall is composed of columnar asperities which are very regular. Figures of a micro-gear, the sidewall of the gear and the columnar asperities microstructure are shown on Fig. 2.1.

Considering two nickel micro-gears fabricated by LIGA, we suppose that these gears are left in contact in a special storage area for a long period of time. We are interested in the evolution with time of the shape of the interface between the two surfaces of these gears. The shape of this interface is a function of the roughness of the two surfaces in contact, and its evolution with time is a function of several phenomena or mechanisms.

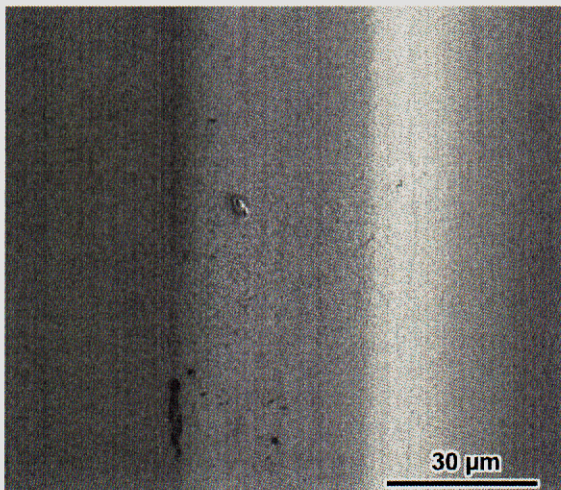
Consider two surfaces in contact in Fig. 2.2. Following Greenwood and Williamson [Greenwood and Williamson, 1966], let $\phi(z)$ be the probability that the height of a particular point on the (top) surface will lie between z and $z + dz$. They found that many real surfaces exhibit a height distribution which is close to the Gaussian probability function. Therefore, we will take the



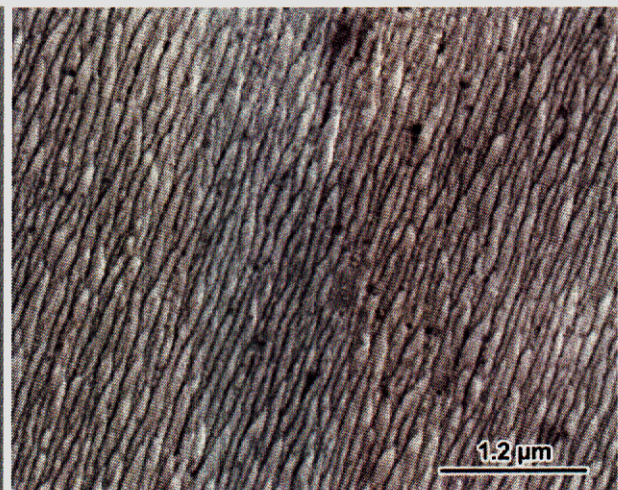
(a) Gear



(b) Gear sidewall



(c) Top of one tooth



(d) Detail of the tooth: columnar microstructure

Figure 2.1: AFM figures of LIGA Micro-Gears. Images taken from S. Prasad, A. Hall and M. Dugger [Prasad et al., 2000]. Note the regular columnar microstructure of the top sidewall's tooth.

following distribution of heights:

$$\phi(z) = \frac{1}{\sigma\sqrt{2\pi}} e^{-z^2/2\sigma^2}$$

where σ is the standard (r.m.s.) deviation from the mean height. Then, at a separation δ between the two surfaces, the total area of contact is given by

$$A(\delta) = N \int_d^\infty f(z_s - \delta)\phi(z_s)dz_s \quad (2.1)$$

and the total nominal pressure by

$$P(\delta) = N \int_d^\infty g(z_s - \delta)\phi(z_s)dz_s \quad (2.2)$$

where f and g are the area of contact and pressure of the local asperities respectively and where N is the number of summits in the nominal surface area.

The problem is now reduced to the study of two asperities in contact. Indeed, when the shape of the surface of contact of two asperities is known, the depth of penetration and the area of contact can be calculated and equations (2.1-2.2) can be evaluated.

In their experiments, Prasad *et al.* analyzed the roughness of the surface of a nickel LIGA micro-gear and showed that the surface of the teeth are formed of columnar asperities, see Fig. 2.1(d). These asperities are 100nm wide and 10nm high in average. When two asperities are in contact,

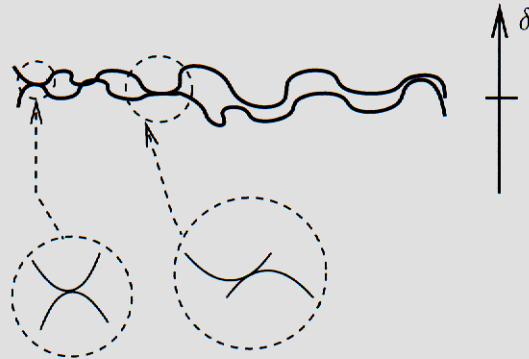


Figure 2.2: Surface roughness and position of asperities

their diameter, dimensions and position relative to the other can be very different and influence their behavior in the aging process. For example, they can be flat, rounded, in phase or out of phase, see Fig. 2.2. These differences in shape and position induce differences in the way they evolve.

The evolution with time of these two asperities in contact depends on several mechanisms. These mechanisms include adhesion, creep, oxidation and diffusion. Their relative importance

CHAPTER 2. STATEMENT OF THE PROBLEM

depends on the external parameters such as temperature, amount of oxygen or other contaminants in the air, characteristics of the material considered etc. As we will see in the following these parameters are intimately related to each other and to the external conditions. The fabrication process of these gears is constantly evolving to improve their performance, and that results in constantly changing product features. This renders difficult a numerical study of their material properties.

2.2 Description of the mechanisms

The mechanisms enumerated above are inter-dependent and act together. Fig 2.3 shows where they are mostly active.

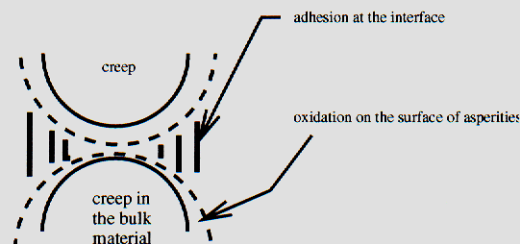


Figure 2.3: Mechanisms involved in the interaction of two surfaces with time. Diffusion influences all areas.

2.2.1 Adhesion

When a nano-scale junction is formed or about to form, adhesion forces affect and have important effects on the behavior of the structure [Persson, 2000], [Redmond et al., 2001] and need to be accounted for. They enhance the attraction exerted by an asperity to the other. Indeed Van der Waals forces can be greater than the contribution to the normal force from the weight of the asperities when the system is at the atomic scale. Adhesion forces tend to increase the contact areas instead of atomic-sized junctions, the smallest junctions may have a radius of order $10 - 100 \text{ \AA}$. This renders impossible individual-atom contact. For example, suppose that the top surface asperity is moved towards a flat substrate. The atoms at the vicinity of the outermost tip atom in contact with the substrate will feel a strong attraction from the substrate. This interaction is either of the Van der Waals nature or of a chemical nature. Energy will be stored in the elastic displacement field at the tip but this increase in the total energy is more than compensated for by the decrease in the energy resulting from the tip-substrate bonding.

2.2.2 Creep

Plastic flow of the material is due to high temperature and load applied to it for a long time [Persson, 2000]. It is characterized by a slow flow of the material and the material behaves as if it were viscous. The theory of visco plasticity describes the flow of matter by creep which, in contrast to plasticity, depends on time [Lemaitre and Chaboche, 1990]. For metals and alloys, it corresponds to mechanisms linked to the movement of dislocations in grains (climb, deviation, polygonization) with superimposed effects of intercrystalline gliding. The effect of creep is to increase the area of contact by flattening the asperities. It may be caused by either a high temperature or localized stress in an asperity.

Several mechanisms can be responsible for creep: the rate-controlling mechanism depends both on the stress level and on the temperature. For temperature below half of the melting point of the metal, the activation energy for creep tends to be lower than the one for self-diffusion. This has been interpreted to be due to diffusion taking place preferentially along dislocations instead of bulk diffusion. For temperature higher than half the melting point of the metal, mechanisms responsible for creep are described as a function of the applied stress.

2.2.3 Oxidation

Among all corrosive substances present in the air or in the stored location of micro gears there is corrosion due to the oxygen. It has important consequences on the behavior of the metal. There exists an empirical power law which relates the thickness of the oxide layer with time t and temperature T , $S(t, T)$ [Scully, 1975], [Wright et al., 1995]. It is given by

$$S(t, T) = k(T)t^n$$

where k and n are mechanism dependent, k depends on temperature T and n on the amount of oxygen considered. The exact evolution with time of the thickness is unknown, a parabolic ($n = 1/2$) or linear ($n = 1$) oxidation are often considered and depends on temperature.

The reaction of a metal with oxygen is extremely rapid even at room temperature since the uptake of oxygen is proportional to the logarithm of the exposure time. The physical and chemical processes occurring during the early stages are complicated, and while several hypotheses have been advanced to explain them, some common phenomenological features have been discerned [Scully, 1975]. A very simple explanation can be summarized as follows. Initially there will be physical adsorption of oxygen molecules on the metal surface. They are relatively loosely bound and the energy of the adsorption process is small. These molecules then dissociate, and the atoms become much more strongly bound by a process of chemisorption which occurs with a much higher energy charge. This chemisorption of oxygen is associated with the movement of a specific number of metal atoms into the plane of the adsorbed oxygen atoms. Together these species form a very stable structure consisting of both negative and positive species which is more stable thermodynamically than bulk oxide. A final thickness formed at room temperature will usually be in the range of 1 – 4 nm (10 – 40 Å), and this is the usual range of thickness. At higher temperature, the range of oxidation ceases to obey a logarithmic law. Growth becomes more rapid

and above some temperature follows a parabolic law. Oxygen atoms are present at the surface of nickel and this influences its behavior when in contact with another asperity. It has been shown in experiments [Yagi-Watanabe et al., 2001] that when Ni(110) clean surface is exposed to the O_2 below $340K$, disordered NiO is formed. An increase of the temperature leads to more complex patterns on the surface and in the bulk nickel.

2.2.4 Diffusion

Diffusion occurs almost in all the mechanisms described earlier; its speed depends strongly on the temperature. It is important in creep and adhesion where atoms move by diffusion from the bulk to the surface, and also in oxidation since atoms of oxygen diffuse from outside into the bulk. Diffusion, being a thermally activated process, shows an exponential temperature dependence. Below half of the melting point temperature of the metal, the diffusion is so low that any deformation mode exclusively dependent on it can effectively be neglected.

2.3 Relations between mechanisms

Adhesion, creep and oxidation act at different level in the material: creep is more important in the bulk, adhesion is more present at the interface between two asperities and oxidation is located at the surface of the material and can penetrate few layers of atoms in the bulk and diffusion is present everywhere Fig. 2.3. Also at the atomic scale, mechanisms like adhesion and creep are in competition with oxidation. Creep and adhesion have the effect of increasing the area of contact between two surfaces whereas oxidation tends to reduce it. These phenomena combine to change the interface between the micro-gears.

Adhesion has a strong effect at the interface between the two surfaces of the asperities through van der Waals forces. It depends on the relative positions of atoms at the interface. Creep acts more globally at the asperity level: it changes its form more through localized stress present in the asperities. Both effect tend to even and smooth the shape of the asperity.

Temperature is an essential parameter in the presence of these mechanisms. High temperatures increase vibrations of atoms and favor creep, oxidation and diffusion mechanisms. Low temperatures tend to stabilize the system by limiting vibrations of atoms and diffusion, and consequently limit creep and oxidation.

2.4 External Conditions

These mechanisms may be important depending on the external conditions applied to the system. It is very difficult to determine precisely what are the temperature, real applied load exerted from the top gear to the bottom one, or the composition of material of the gear, etc. However, some aging experiments done by Yang *et al.* [Yang and Kelly, 2002] are currently underway and have the objective of answering some of these questions with specific constrained external conditions.

The current properties of these gears are the following:

1. They are stored in a special nitrogen environment which prevents corrosion, and they are left in contact one on top of the other and pinned. The contact is maintained by spring forces.
2. The temperature is far below half of the melting point of nickel, and gears are not intended to be used in extreme temperatures conditions.
3. They are constructed of almost pure nickel, although some residual materials such as PMMA are often present at the top of the teeth of the gears due to the construction procedure. Also a precise analysis of the oxygen layer at the surface of the gears has not been completed.
4. Nickel does not react readily with oxygen, and only a few atomic layers at the surface can be contaminated with oxide. The oxide layer is thin and atoms of oxygen and nickel are arranged in a disorderly manner at the surface of the gears. There are few or no oxygen atoms in the bulk.

In this report we model the behavior of the interface of the gears in recognition of some of the phenomena described in this chapter. We do not intend to model the evolution of these phenomena with time specifically but rather analyze our results by keeping these phenomena in mind. We will be mainly concerned by the adhesion mechanism since it is the one really observed in the numerical simulations. Phenomena such as creep and oxidation are not accounted for in the model presented in this paper, they will be the object of study of a future work.

CHAPTER 2. STATEMENT OF THE PROBLEM

This page intentionally left blank.

Chapter 3

Simulation Methods

In this chapter, we introduce our method to study aging and compute reaction forces of one asperity on the other. In the previous chapter, we discussed how the study of two asperities can lead to the understanding of macroscopic properties of the interface between two gears using Greenwood and Williamson's surface theory. A brief review of particle simulation methods such as molecular dynamics and energy minimization using a conjugate gradient method is included in the present chapter. Specific details such as boundary conditions and particle ensembles are discussed and particularized to the system in consideration.

Numerical aspects of this work have been implemented in the code ParaDyn developed by S. Plimpton [Plimpton, 1995]. ParaDyn is a parallel molecular dynamics and energy minimization code. The potential used in ParaDyn is based on the Embedded Atom Method (EAM) developed by Daw, Baskes and Foiles [Daw and Baskes, 1983, Daw and Baskes, 1984, Foiles et al., 1986, Daw, 1989].

3.1 Equilibrium and Energy Minimization

Macroscopic equilibrium requires system-wide mechanical, thermal and chemical equilibrium and it is assumed that a steady state is reached for an isolated system after a long time. By definition, equilibrium is reached when no more changes in the properties, e.g. momentum in the case of mechanical equilibrium or temperature in the case of thermal equilibrium, of the system are noticed. No changes in system momentum or temperature, however, does not imply that there are no microscopic vibrations at the atomic level. Actually, given a kinetic definition of temperature, microscopic vibrations are required for a non-zero system temperature and, in equilibrium, many microstates, i.e. configurations of atomic positions and momenta, can be associated with a given macrostate of the system. The temperature and entropy of the system provide measures of how many degenerate microstates yield a given value of energy. Like the fact that there are typically many microstates associated with a given macrostate, there are many macrostates associated with a particular system. Of these many possible macrostates, there can exist a "most favorable" one, statistically speaking, associated with lowest possible energy the system can attain given its external environment.

In this report, we are interested in the state of the system after 20 years of rest. After this dormancy period, the system is either in equilibrium or in a metastable state. In either case, the energy is minimized. This energy minimum is the global minimum in the case of equilibrium and is a local minimum in a case of a metastable state. We make the assumption that the state in which the system will be after 20 years corresponds to the minimum energy state. This is equivalent to assume that either the system is at zero temperature or thermally insulated or that the term corresponding to the temperature and entropy in the free energy is negligible. The conditions in which the system is stored, in a liquid nitrogen environment, lead us to assume that it is insulated thermally.

It should be noted however that the assumption that the system is thermally isolated is not essential in this problem since, for solids, the main effect of the presence of medium to high temperatures on the energy is thermal expansion. For this reason, regardless of the condition of thermo insulation, the knowledge of the ground state of the system is an important information of the dormant system.

Also if instead of computing the actual state of the system after dormancy, we are able to compute the global energy minimum or a local minimum of the system then we can give an estimate of the upper bound value of the adhesion force due to the interface constructed between the two micro-gears in contact with time. The global energy minimum corresponds to the most probable position of the atoms after dormancy.

In this report, we use molecular statics (energy minimization) and molecular dynamics simulations to study the influence of the shape and offsets of two asperities on the evolution of the surface with time. The method we used for energy minimization permits us to determine local energy minima and not global energy minimum. In chapter 6, we will explain how it is possible to find the global energy minimum of the system, which will be the objective of future work.

3.2 Implementation of atomistic simulation methods

This section discusses the computational techniques used for simulations of material deformation at the atomic scale. Among the important concepts to understand are the time step limitations and the type of boundary conditions applied to the system. This section also presents a description of the methods used to study aging and adhesion.

3.2.1 Molecular dynamics

Description of the molecular dynamics method

Molecular dynamics is perhaps the most straightforward type of simulation method used by researchers to analyze materials problems. It involves deriving the equations of motion for a system comprised of a large number of particles, which results in a set of coupled ordinary differential equations, and solving these equations by discretization of time and approximation of time derivatives. The governing equation of motion is Newton's 2nd law,

$$\mathbf{F}^\alpha = m_\alpha \ddot{\mathbf{x}}^\alpha. \quad (3.1)$$

3.2. IMPLEMENTATION OF ATOMISTIC SIMULATION METHODS

In this expression, \mathbf{F}^α denotes the force acting on particle α , m_α denotes that particle's mass, and \mathbf{x}^α denotes the the particle's position.

The equations of motion can also be derived using more advanced methods such as Hamiltonian dynamics. This type of mechanics uses a function of particle positions and momenta which is known to be constant for a particular system. Such is the case for an isolated system of particles in which that function, the Hamiltonian \mathcal{H} , is known to be the total (kinetic plus potential) energy of the system.

$$\mathcal{H} = \sum_{\alpha=1}^N \frac{p_k^\alpha p_k^\alpha}{2m_\alpha} + \mathcal{U}(\mathbf{x}^N) = E. \quad (3.2)$$

Here, p_k^α denotes the momentum of particle α in the k^{th} direction,

$$\mathbf{p}^\alpha = m_\alpha \dot{\mathbf{x}}^\alpha, \quad (3.3)$$

\mathcal{U} denotes the potential energy of the system of N particles, and E is the total energy of the system, a constant. The differentiation of the Hamiltonian with respect to time and for an isolated system equals zero, and reproduces Newton's 2nd law (3.1) provided the force acting on particle α is conservative,

$$\mathbf{F}^\alpha = -\frac{\partial \mathcal{U}}{\partial \mathbf{x}^\alpha}, \quad (3.4)$$

which is true for an isolated system of particles.

The equation of motion (3.1) of particle α is coupled to the equations of motion of all the other particles in the system ($\beta = 1, 2, \dots, \alpha - 1, \alpha + 1, \dots, N$) through the conservative forces (3.4) present. Thus, a closed-form solution that defines the particle's motion for all time generally cannot be found. Instead, the coupled equations of motion are discretized in time; positions are found at a specific time step $t = n\Delta t$ based on positions and velocities at previous time steps. This is known as the finite-difference method. A commonly used finite-difference algorithm is the one developed by Gear [Gear, 1971, Haile, 1992], which uses a Taylor series expansion with higher-order derivatives to predict future motion, relying on force calculations to correct these predictions.

An important feature of this algorithm is how large to make the time step. Naturally, it would be desirable to have the time step be arbitrarily large, so phenomena that occur over any time scale could be modeled. However, the particle forces at a given time step are really average values over this increment, so the time step cannot be too large. This limitation is best seen by looking at the variation of the total energy of an isolated system. For such a system this variation should be identically zero, but realistically the variation will be finite with a monotonic dependence on the time step.

A further complication arises from the dimensional units of the system being simulated. When the time step is said to be "too large" or "too small", this has to be interpreted with respect to a characteristic value of time intrinsic to the material system. Such a dimensional factor of time is calculated from the quantity

$$\tau = \sigma \sqrt{\frac{m}{\epsilon}}. \quad (3.5)$$

In multi-particle systems where the particles are atoms, the values of σ , m and ϵ represent bond length, atomic mass, and cohesive energy of a bulk atom, respectively. The time step can then be expressed in the non dimensional form

$$\Delta t^* = \frac{\Delta t}{\tau}. \quad (3.6)$$

For this research a value of $\tau = 10^{-12}$ sec was chosen. Once this time scale is chosen, an analysis of the variation of system energy is performed to determine an acceptable value of Δt^* . Typically, this value was chosen to be 0.001 in numerical examples of chapter 4

Application of the method to compute the reaction force

Suppose that the system is in the dormancy phase and we want to re-activate it. Over time, the surfaces of each nickel asperity will have bonded and a nanoscale junction will have formed between them. In order to implement the adhesion exerted from one asperity on the other one, we compute the reaction force of the body formed by one asperity on the other body formed by the other asperity. It is given by

$$R_{T \rightarrow B} = \sum_{i \in \mathcal{T}} F_i = -R_{B \rightarrow T}$$

where \mathcal{T} are the atoms located in the top asperity. This force is a measure of the amount of work necessary to pull the two asperities apart if they have joined.

Molecular dynamics is used to evaluate this force. At each time step Δt^* , an imposed displacement is exerted on each asperity to model their separation and the force is evaluated. When this force vanishes, the top asperity and the bottom one are not connected anymore, and the junction has broken.

3.2.2 Energy minimization techniques

Monte Carlo methods and importance sampling

Monte Carlo methods [Leach, 2000], [Frenkel and Smit, 2002] are primarily used to calculate properties of the system accurately such as thermodynamic quantities, e.g. average internal energy, heat capacity etc. They are not used to devise the positions of the atoms at equilibrium. A Monte Carlo simulation generates configurations of a system by making random changes to the positions of the species present, together with their orientations and conformations where appropriate. Many computer algorithms are said to use a “Monte-Carlo method” meaning that some kind of random sampling is employed. In molecular simulations, “Monte Carlo” is almost always used to refer to methods that use a technique called importance sampling. Importance sampling methods are able to generate states of low energy.

When we talk about Monte Carlo moves in the following, we really mean importance sampling. Our idea to find the global minimum of the system is to use a specific random search method composed of a regular energy minimization technique plus a smart choice of the random changes to the positions of the atoms. Refer to Chapter 6 for more details.

Description of the energy minimization method

Although molecular dynamics gives interesting and useful information about the motion of atomic systems, it is limited by the time scale requirements of modeling atoms. Some material phenomena are observed to occur over time scales which are outside of this range. The dormancy phase is an obvious example. For these cases, methods of energy minimization are used. These types of simulations determine particle configurations with lower potential energy, searching in an unphysical way which cannot necessarily be tied to a time scale. One such method is the conjugate gradient method [Vanderplaats, 1984, Press, 1989, Shewchuk, 1994], which determines specific trajectories for the system's particles which are conjugate to all previous trajectories.

Application to the study of aging

We look for the energy minimum of the system and we make the hypothesis that they will be the states after dormancy since they are energetically favorable over all other states. The most favorable state being the global energy minimum. This state can be evaluated using conformational analysis. It consists of doing an energy minimization coupled with Monte Carlo smart moves. This method is a way to reach more states of the system and not get stuck in a local minimum. The idea behind these moves is to explore more states of the system since they all have a non-vanishing likelihood to be occupied and while visiting them to record their energy.

In this report, a simple energy minimization via conjugate gradient methods is performed. More sophisticated techniques will be studied later. Local minimum are statistically likely states of the system after the dormancy period. A search of these states is done here, and this gives a first insight in the underlying problem of the method.

3.3 Description of the numerical model

3.3.1 Details of implementation: boundary conditions

Two options available are rigid boundary conditions and periodic boundary conditions. Rigid boundaries stem from walls beyond which atoms cannot travel. They are usually implemented by restricting a layer or two of atoms bordering the walls to have limited degrees of freedom. However, energies and forces of atoms that make up the rigid boundary are not equivalent to bulk atom energies and forces. Thus, calculations of energy and stress for such a system might be misinterpreted.

More commonly used in simulations are periodic boundary conditions. If an atom is moved beyond the system's boundaries, then its position is recalculated with the appropriate length subtracted, effectively moving the atom to other side of the simulation region. In this way, it can be considered that the atom has left the simulation region while its periodic image has entered it. Atoms near the periodic boundaries in these systems have the same energies and forces as bulk atoms because they effectively "feel" the periodic images of other atoms as their nearest neighbors. Thus, periodic boundary conditions allow a small simulation region with a limited number

of particles to successfully model bulk material, enabling calculation of bulk properties.

3.3.2 Specific details of the system

The special microstructure observed by Prasad *et al.* [Prasad *et al.*, 2000] is regular, periodic and small: their average dimensions are on the order of nanometers. A good description of the asperities of this microstructure is a half cylindrical shape with a rigid boundary in the z direction with periodic conditions in the x and y directions (see Fig. 3.1). By periodicity, the full microstructure can be recovered.

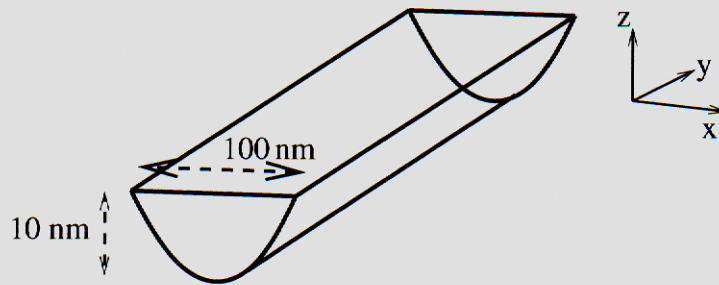


Figure 3.1: Description of the studied system

The system studied is composed of two asperities made of pure nickel and forming perfect fcc lattices. This ideal case does not reflect the actual microstructure which has many defects such as oxygen atoms, PMMA residues etc. The parameters of the nickel metal for the EAM potential we used are those used in [Baskes, 1997].

We consider two of these half cylindrical shape close to each other, one on top of the other modeling two asperities in contact. The form of these asperities is represented by two parameters. The first one is the radius R of an asperity. It is shown on Fig. 3.2. It represents the height and flatness of the asperities. The larger R is, the flatter the asperity.

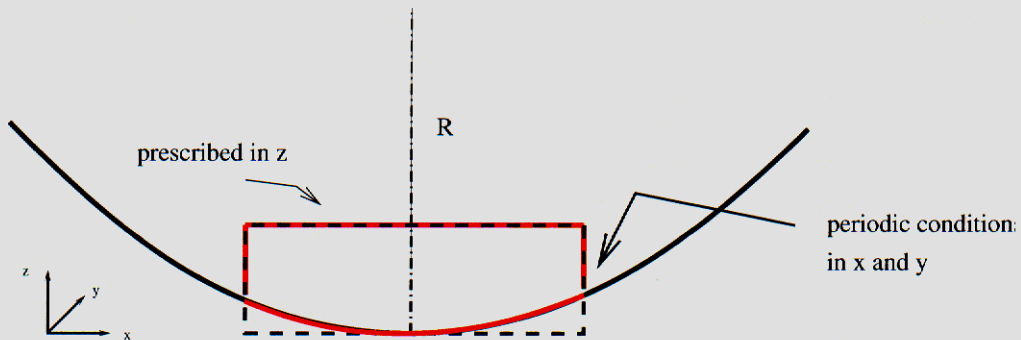


Figure 3.2: Definition of the radius R and boundary conditions. The asperity is shown in red.

3.3. DESCRIPTION OF THE NUMERICAL MODEL

The second parameter is the offset of the top asperity with respect to the bottom one. The two asperities can be right on top of each other or shifted. This makes a difference in how many atoms actually see the others. These parameters will be varied in our calculations.

It is not so clear what should be the right atomic distance of separation of the two asperities. From a numerical point of view, atoms in one asperity have to be close enough to see atoms in the other asperity. That is to say that the corresponding pair of atoms's interaction has to be considered by the algorithm. We chose to separate the two asperities by a small distance corresponding to one atomic layer. At the scale of the micro-gears, they can then be considered to be in contact.

This page intentionally left blank.

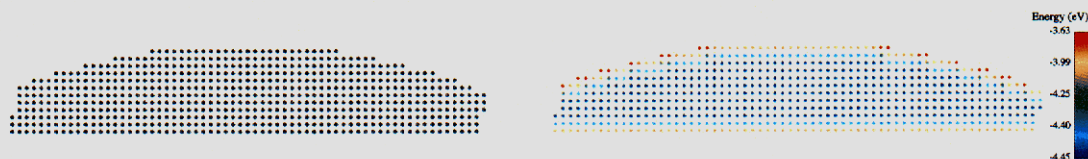
Chapter 4

Simulation of aging and adhesion forces

In this chapter, we apply the theory explained previously on test cases. Although the size of an average asperity is small enough to run direct atomistics simulation, it remains expensive and we first present some results for a system scaled to 1/10th the size of an actual physical system. Some of the results for this case are valid at larger scales. We also show simulation results for a system with the same dimensions as an actual physical structure.

4.1 Numerical simulation of aging via energy minimization

The first simulation we studied is that of a relaxation of a simple asperity of pure nickel. Fig. 4.1 shows the initial mesh of atoms and the positions of the atoms after relaxation as well as their potential energy. When atoms of nickel are at rest, their energy is -4.45eV . The energy that is represented is the potential energy per atom. This domain contains approximately 4,000 atoms, corresponding to only 1/10th of the actual size of an asperity. We observe on Fig. 4.1(b) that the effect of imposing a rigid boundary in the z direction is to have atoms located at the boundary with a high energy although they should be at the same energy level as the ones in the bulk. We can also see on Fig. 4.1(b) that the surface tends to relax inward due to minimization of the surface energy which is a known property of metals. The embedded atom method captures the phenomena correctly.



(a) Initial structure: simple bump of nickel

(b) Potential energy after minimization

Figure 4.1: Relaxation of a simple bump of nickel

We study now the evolution of two asperities separated by a small distance. We want to know the roughness effect on bonding, i.e. whether it corresponds to full cohesion of lattices or stretching of the bonds. For this purpose, we simulate how the radius of the asperities and the offset influence the bonded region. We chose three different values of R , see Fig. 3.2 (denoted by $R/2$, R and $2R$) and three possible offsets of the top asperities with respect to the bottom one (offset of $1/3$ of period, $1/2$ and no offset). In what follows $R = 5\text{nm}$ and the dimensions are $10 \times 3 \times 1\text{nm}$. This represents approximately $1/10\text{th}$ of the actual size of an asperity which size is usually of the order of $100 \times 3 \times 10\text{nm}$. Each case gives a different relaxation and contains approximately 8,000 atoms. A review of all initial states and final relaxations is shown on Figs. 4.2 - 4.4. On the left of each figure is the initial configuration while on the right the final configuration with the atoms colored to their value of potential energy.

The energy represented on Figs. 4.2 - 4.4 is the energy per atom. Atoms with higher energies are located on the free surface of the system. The rigid boundary conditions in the z direction have the consequences of increasing their energy.

It is interesting to note in these figures that a nano-scale junction located at the interface between the asperities is formed in almost all cases. This junction corresponds to atoms which have bonded and in most cases to a reestablishment of the perfect lattice between atoms at the interface. Only atoms which are sufficiently close to each other bond. Atoms located on the free surface but not at the interface do not interact but have a higher energy because they are located on a free surface. In the case of two asperities with no offset (Fig. 4.4), we remark that atoms at the interface have not formed a full cohesion but have been stretched from their initial position. In all other cases (Fig. 4.2- 4.3) the perfect lattice has been reformed, minimizing the energy of the system. The atoms that are actually reacting are the ones within the predefined cut off distance. The atoms in the bulk are just compressed towards the interface. Their energy corresponds to atoms at rest.

For all these examples, most of the phenomena happen at the interface between two asperities. Atoms are displaced at the surface and at the interface but they do not move much in the bulk. The energy also is higher at the surface than in the bulk. The numerical solution favors the minimization of the surface over the bulk and tends to reconstitute perfect lattices where it can.

4.1. NUMERICAL SIMULATION OF AGING VIA ENERGY MINIMIZATION

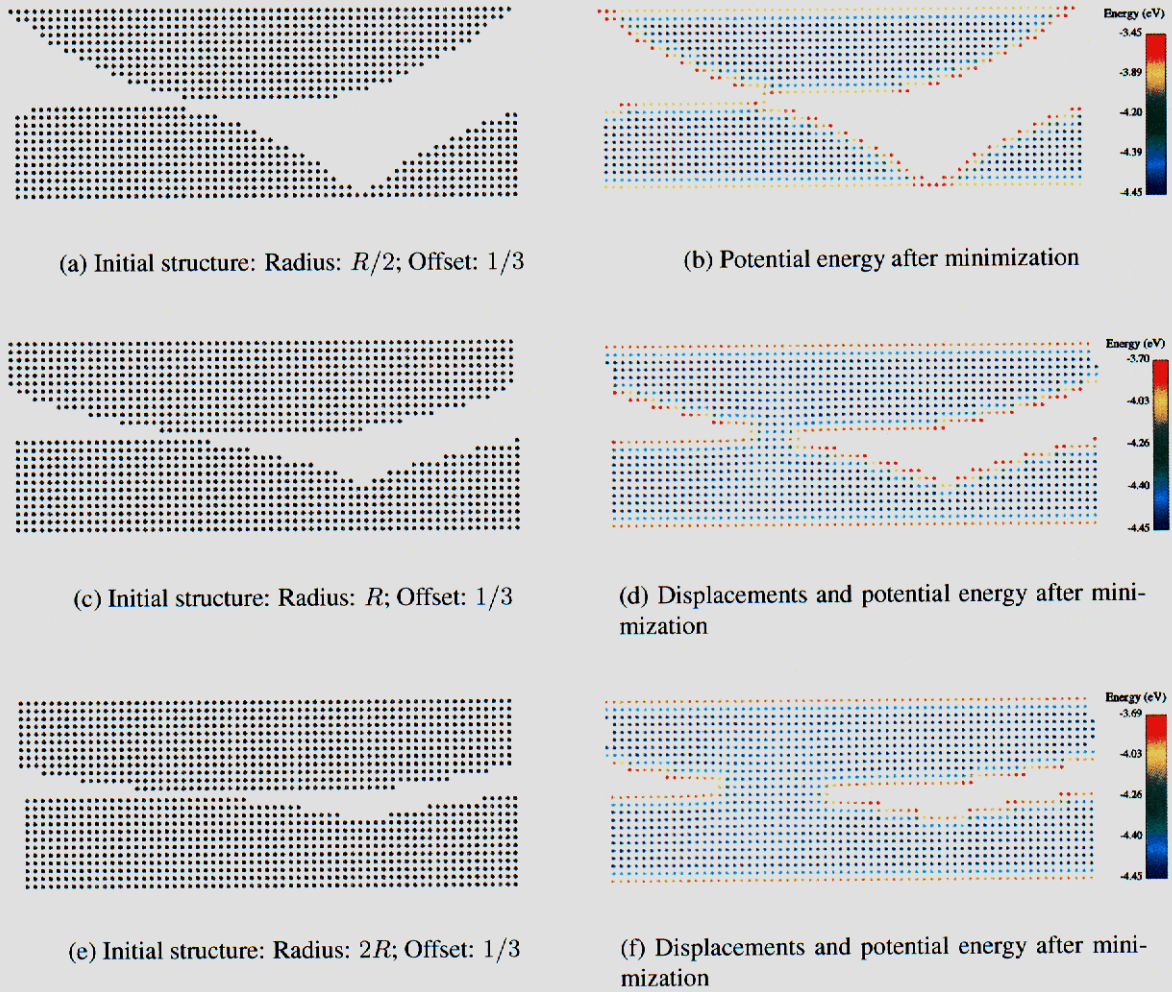
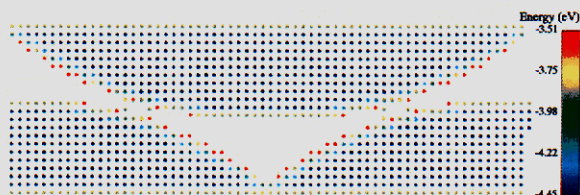


Figure 4.2: Initial and final state of the atoms after aging



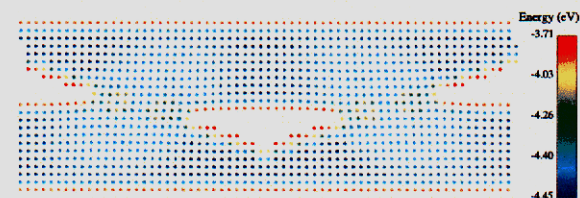
(a) Initial structure: Radius: $R/2$; Offset: $1/2$



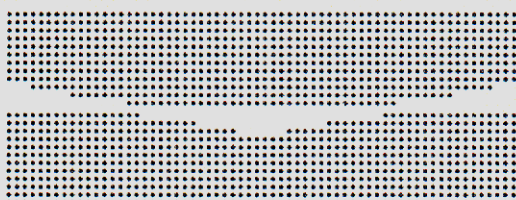
(b) Displacements and potential energy after minimization



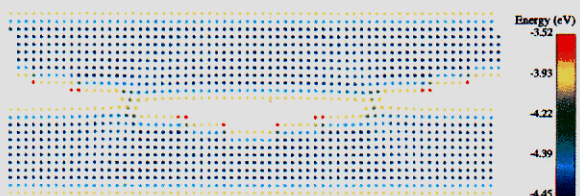
(c) Initial structure: Radius: R ; Offset: $1/2$



(d) Displacements and potential energy after minimization



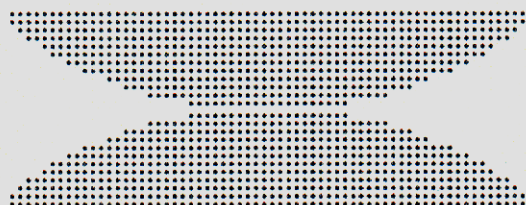
(e) Initial structure: Radius: $2R$; Offset: $1/2$



(f) Displacements and potential energy after minimization

Figure 4.3: Initial and final state of the atoms after aging

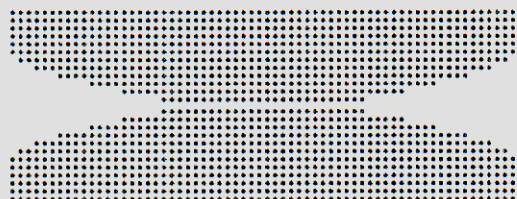
4.1. NUMERICAL SIMULATION OF AGING VIA ENERGY MINIMIZATION



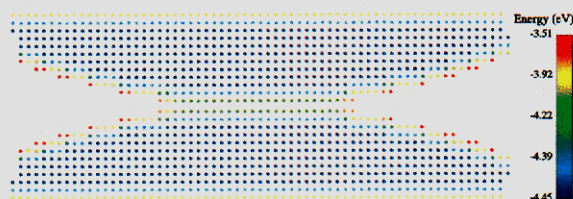
(a) Initial structure: Radius: $R/2$; No offset



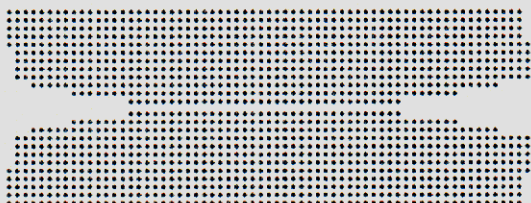
(b) Displacements and potential energy after minimization



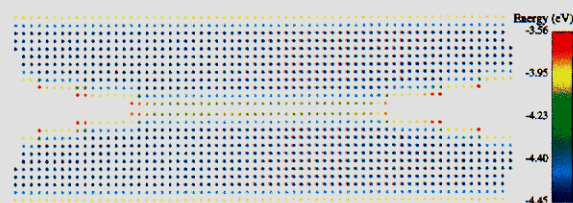
(c) Initial structure: Radius: R ; No offset



(d) Displacements and potential energy after minimization



(e) Initial structure: Radius: $2R$; No offset



(f) Displacements and potential energy after minimization

Figure 4.4: Initial and final state of the atoms after aging

4.2 Numerical simulation of adhesion

In this section, we suppose that the state of the system after dormancy is the state found in section 4.1 and that it is time to reactivate the gears and see if they function again. We want to compute the force necessary to pull both surfaces apart and, if necessary, break the junction which may have been built during the minimization step. The reaction force exerted from the top asperity to the bottom one gives an estimate of how difficult it can be to break the junction.

As explained in the previous chapter, the reaction force exerted from one asperity to the other can be estimated using molecular dynamics simulation. At each time step of the simulation we impose a displacement to top and bottom layers of the asperity of same intensity but in opposite direction to separate them. Then we record the reaction force at each time step to measure the force necessary to break the junction up.

Snapshots of the MD simulation are shown on Fig. 4.5 for the case of a radius R and an offset of one half (see corresponding minimum of energy on Fig. 4.3). At each time step ($\Delta t^* = 10^{-3}$), an imposed displacement on each asperity in the $\pm z$ directions is prescribed leading to the separation of the asperities and the breaking of the bond at the nano-scale junction. The total number of time steps for this simulation was 55,000. We varied the rate of displacement and we show in Fig. 4.5 a simulation corresponding to a rate of $7 \text{ \AA}/ms$.

We have also calculated the reaction force of the top asperity on the bottom one as well as the total energy during the simulation. Fig. 4.6(a) shows the reaction force for different imposed displacements rates and Fig. 4.6(b) shows the corresponding total energy per atom, which is the sum of the potential and kinetic energies.

The global trend of the computed reaction force shows that it starts by increasing up to a maximum corresponding to the breaking up of the junction and then decreases towards zero. The value of the displacement where the junction breaks can be recorded from Fig. 4.6(a). After the separation, the reaction force vanishes. Atoms located at the free surface have a high energy because they are close to the one they have just separated from.

We observe on Fig. 4.6(a) and Fig. 4.6(b) that for rate of displacement of the order of the Angstroms/millisecond, the reaction force and the energy are independent of the rate of displacement, their corresponding curves overlap. When this rate increases, we observe on Fig. 4.7(a) and Fig. 4.7(b), that it is not true anymore: for rates of displacement of the order of the Angstroms/centisecond, the reaction force and the energy does depend on the rate of displacement, and their corresponding curves do not overlap anymore. However increasing the rate is equivalent to increasing the time step of the molecular dynamics simulation and this leads to numerical instabilities. What we can conclude from the curves of Fig. 4.6(a) and Fig. 4.6(b) is that for small rates, the reaction force and the energy do not vary much with increasing rates.

We have calculated the reaction force and energy for all the other radii and offsets described previously in section 4.1. Fig. 4.8(a) shows a comparison of reaction forces for three different radii for the case of an offset of one third corresponding to the dormancy phase of Figs. 4.2(a)-(c). Fig. 4.8(b) shows a comparison of the reaction force for three different radius for the case of no offset. These reaction forces correspond to the dormancy phase shown on Figs. 4.4(a)-(c) and are for a displacement of $7 \text{ \AA}/ms$.

4.3. STUDY OF A SIMULATED SYSTEM WITH DIMENSIONS OF A PHYSICAL SYSTEM

For the first comparison (Fig. 4.8(a)), it is clear that the larger the bonded junction, the higher the reaction force. It shows that the bigger the junction the more difficult it is to separate the two asperities. This can be explained by the fact that many more atoms have to be separated, and this increases the energy to break the junction.

The reaction force necessary to separate the two asperities corresponds to the force necessary to break the bonds at the interface. On Figs. 4.2(a)-(c), the bonded junction increases with increasing radius and the reaction force curves of Fig. 4.8(a) follows the same trend.

On the second comparison (Fig. 4.8(b)), we observe a different phenomena. In the dormancy phase, the two junctions have not bonded (see Figs. 4.4(a)-(c)) and atoms have only been stretched from their initial positions. The corresponding reaction force curves show that to separate the junction, a similar force should be applied. This force oscillates much more in comparison to the one for an offset of $1/3$. These oscillations correspond to individual atoms recovering their initial position in the perfect lattice and they oscillate until they have returned to their more stable position.

4.3 Study of a simulated system with dimensions of a physical system

All the previous numerical results were done using $1/10$ th of the actual size of an average asperity but a problem with dimensions of a physical system can also be solved by the same techniques. Several interesting details appear in this case.

The results of the minimization process is shown on Fig. 4.9. A close-up of the initial and final positions of the atoms as well as the energy per atom in eV is shown on Fig. 4.10 which shows more details of the nano-scale junction. This case was simulated using approximately 170,000 atoms corresponding to a $100 \times 3 \times 10$ nm size asperity. This minimization took approximately 6 hours on a one processor PC.

We can observe in this simulation more details than in the smaller system. The nano-scale junction formed at the interface between the two asperities is much more complex than the one obtained from the scaled case of Fig. 4.3(b) which is the closest comparison with this simulation. Many more interactions are observed in this case since more atoms are seeing each other. Indeed on Fig. 4.10, details of the nano-scale junction are interesting to observe. The perfect lattice has not been reconstructed completely, instead, distortions in the lattice are observed. This phenomenon was not observed in the small scaled numerical simulations.

The form of the nano-scale junction is very particular: it exhibits a large contact area but an imperfect lattice, many defects in the lattice can be observed on the close-up of Fig. 4.10(b). As noted earlier (see chapter 2, section 2.2.1), the adhesion force tends to increase the contact areas instead of individual-atom contacts, and this is what is observed on Fig. 4.10(b): a large area of contact is present at the surface of the asperities. The presence of defects in the lattice at the junction is due to the initial position of the atoms as shown on Fig. 4.10(a). Atoms at the interface of each asperity do not have all their surrounding neighbors since they are located on the free surface, and they are attracted by the atoms close to them located on the other surface. These

atoms located on each surface are not always perfectly aligned, and their attraction results in the details observed on Fig. 4.10(b).

A molecular dynamics simulation has also been performed for this case in order to separate the formed junction (Fig. 4.9) and compute the reaction force and the energy necessary to break it up. A close-up of the last step of the simulation corresponding to full separation is shown on Fig. 4.11. The reaction force and the energy per atom are shown on Fig. 4.12.

We can observe in Fig. 4.11 that the perfect lattice has been reconstructed completely although some atoms have not returned to their initial positions. Also we observe from the curves on Fig. 4.12 that they follow the same trend as the scaled case. However, they do not collapse with them. The reasons are that in the larger case, many different complex interactions appear compared to the smaller case. The junction is more difficult to break, and it necessitates more energy and a longer reaction force. This suggests that the bigger the surface in contact, the higher the adhesion force.

The form of the interface after relaxation and after having been pulled apart have similarities with crack formation and propagation. The force shown on Fig. 4.12 may be interpreted as a characterization of the rupture process occurring in the crack-tip fracture process zone.

4.3. STUDY OF A SIMULATED SYSTEM WITH DIMENSIONS OF A PHYSICAL SYSTEM

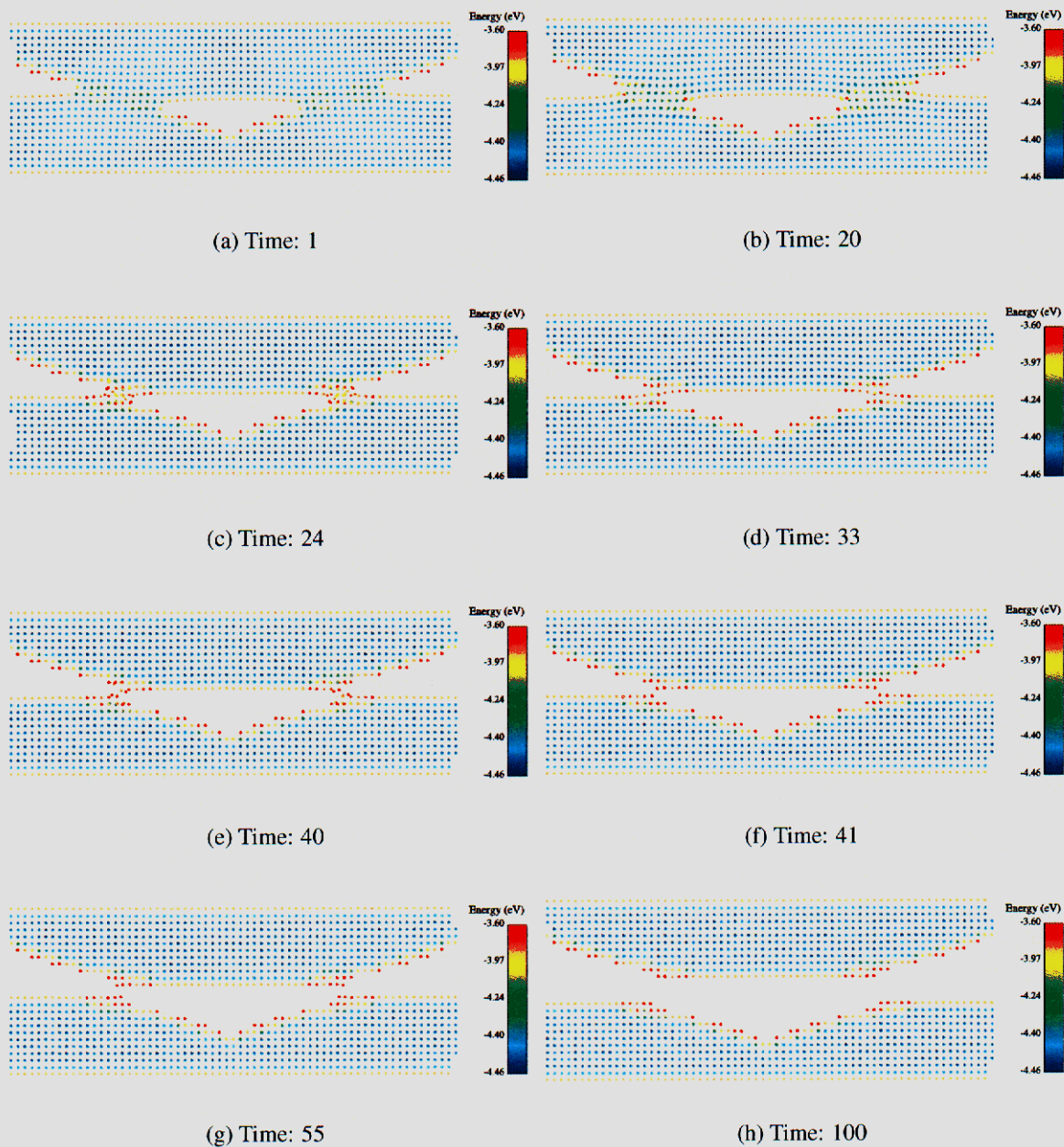
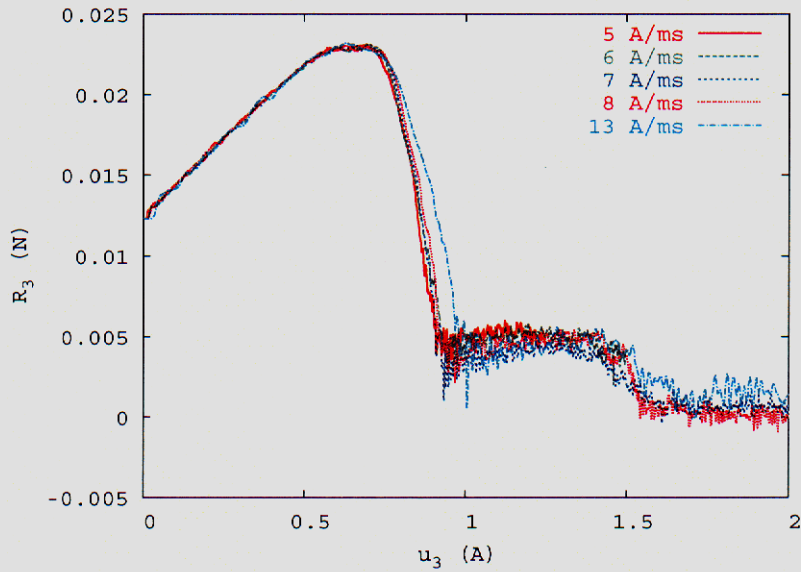
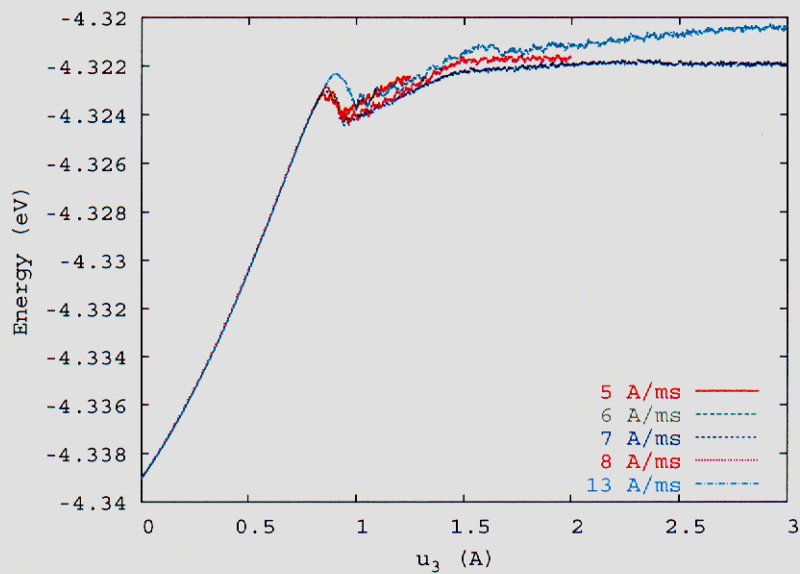


Figure 4.5: Snapshots of MD simulation of pulled-apart force



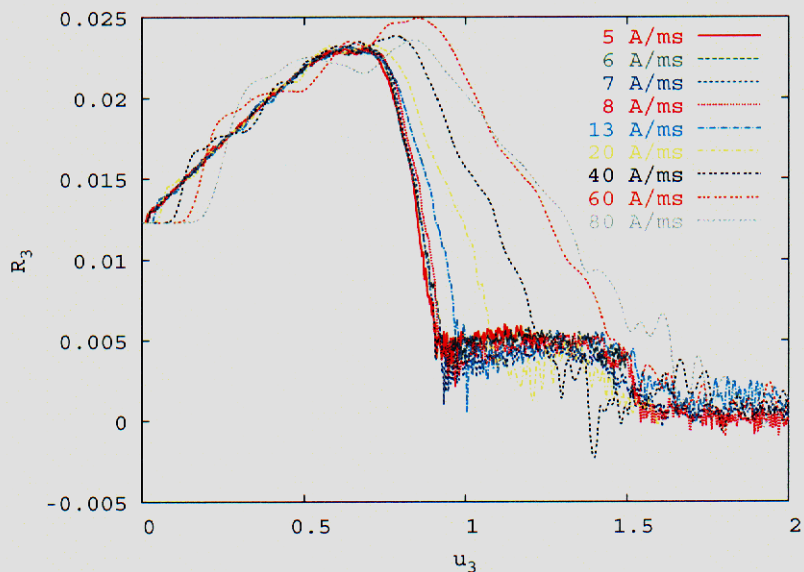
(a) Displacement vs. Reaction force of the top asperity on the bottom one for rates on the order of Angstroms/millisecond.



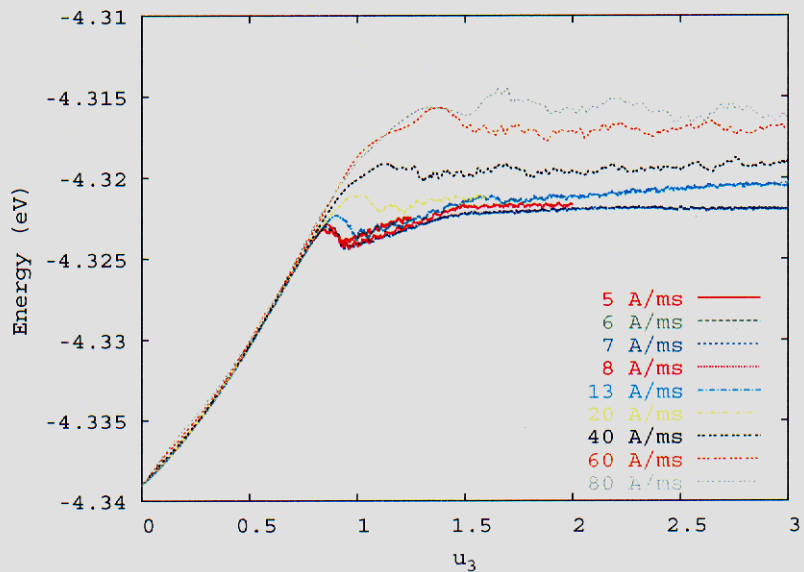
(b) Displacement vs. total energy for rates on the order of the Angstroms/millisecond.

Figure 4.6: Reaction force on top and Energy per atom on the bottom for an offset of $1/2$. Note that for this range of rates, the curves overlap.

4.3. STUDY OF A SIMULATED SYSTEM WITH DIMENSIONS OF A PHYSICAL SYSTEM

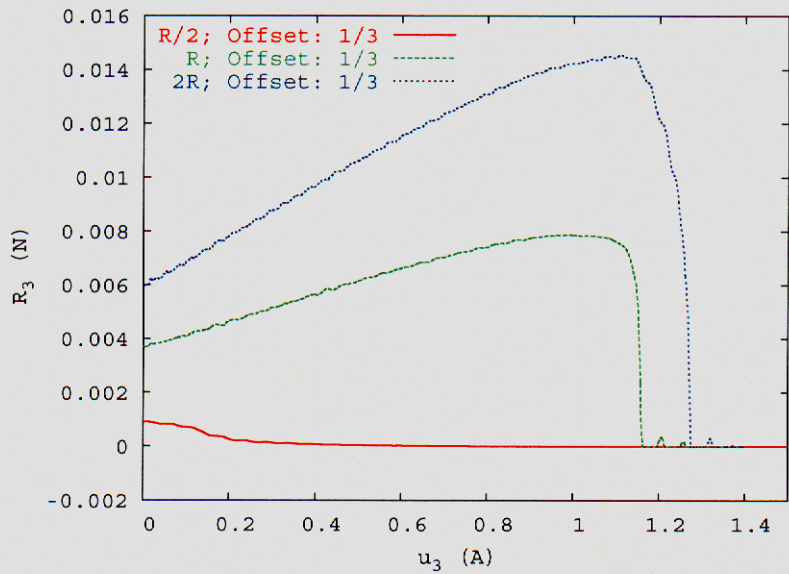


(a) Displacement vs. Reaction force of the top asperity on the bottom one for rates on the order of Angstroms/centisecond.

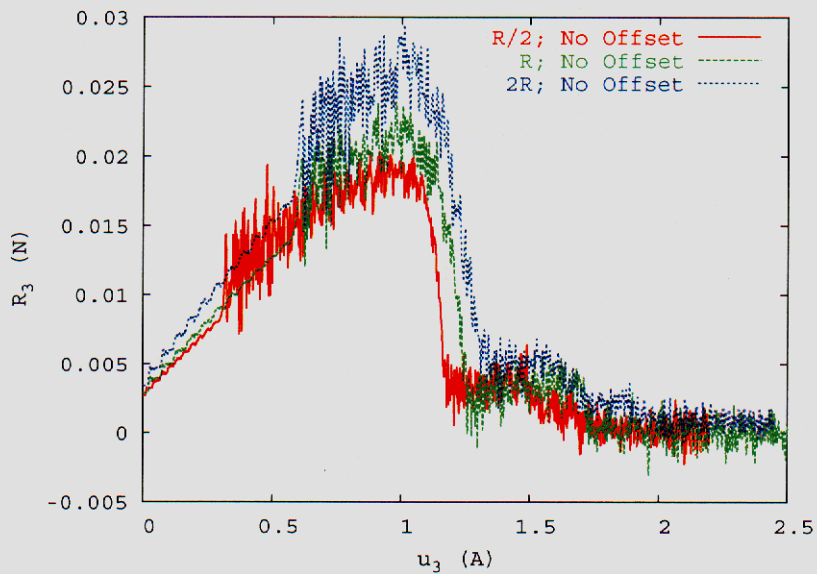


(b) Displacement vs. total energy for rates on the order of Angstroms/centisecond.

Figure 4.7: Reaction force on top and Energy per atom on the bottom for an offset of $1/2$. Note that for this range of rates, the curves do not overlap.



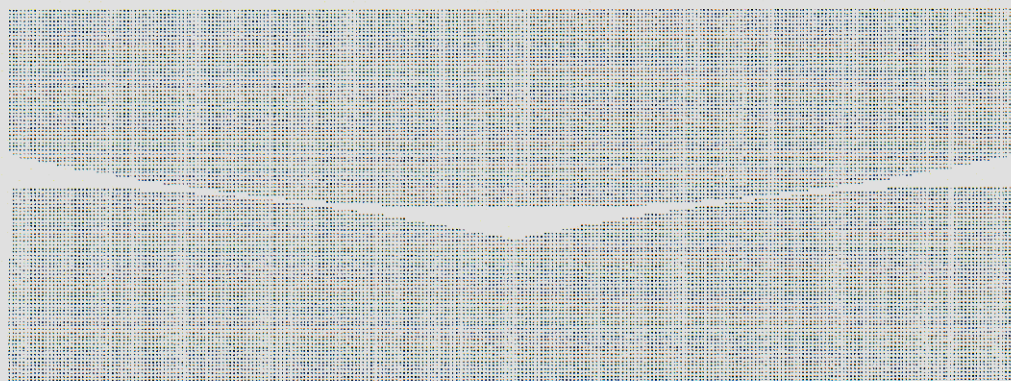
(a) Displacement vs. Reaction force for an offset of $1/3$. Bonds formed during aging and broke during separation simulation.



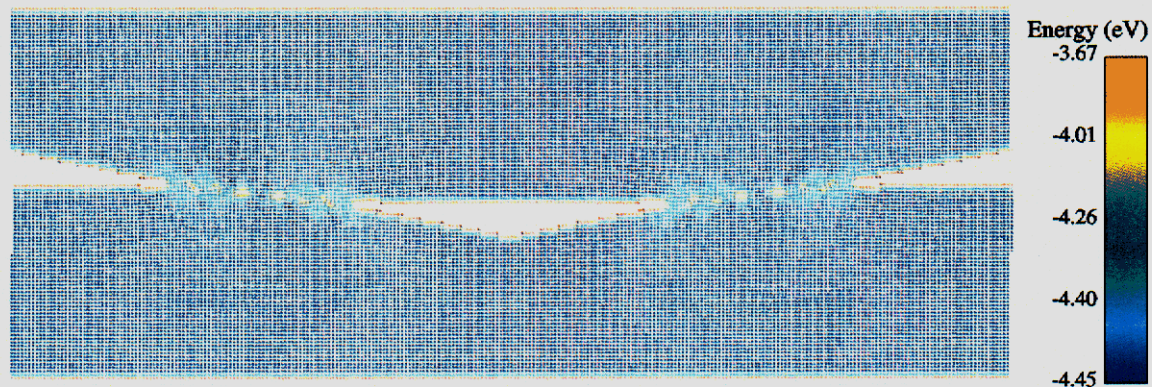
(b) Displacement vs. Reaction force for no offset. Bonds stretched during aging and went back during separation simulation. Note oscillations of the force.

Figure 4.8: Reaction force for special offsets at $7 \text{ \AA}/m.s.$

4.3. STUDY OF A SIMULATED SYSTEM WITH DIMENSIONS OF A PHYSICAL SYSTEM



(a) Initial structure: Radius: R ; Offset: $1/2$

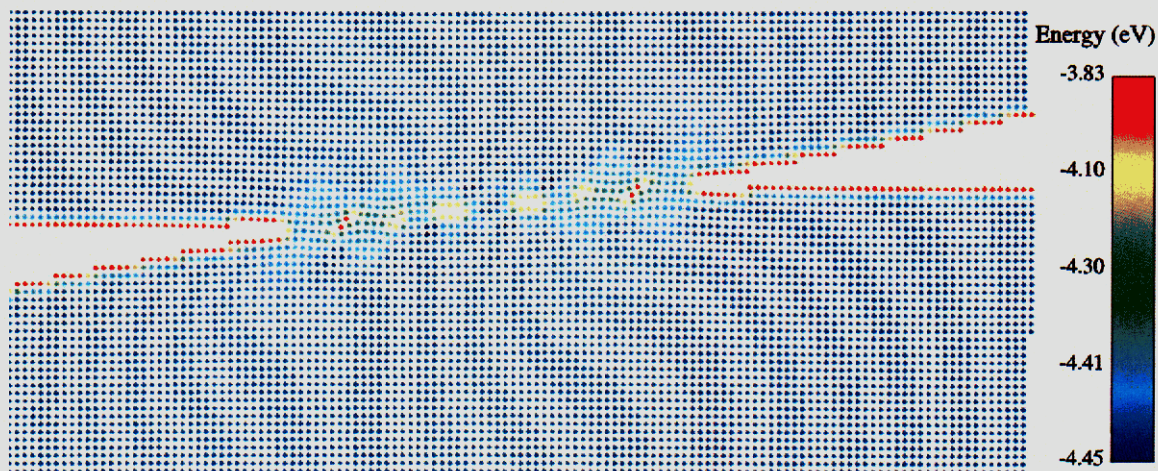


(b) Close-up of the initial and final positions of atoms

Figure 4.9: Final state of the atoms after aging for a physical dimension problem



(a) Close-up of the initial state



(b) Close-up of the final state

Figure 4.10: Close-up of the final state of the atoms after aging for a physical dimension problem

4.3. STUDY OF A SIMULATED SYSTEM WITH DIMENSIONS OF A PHYSICAL SYSTEM

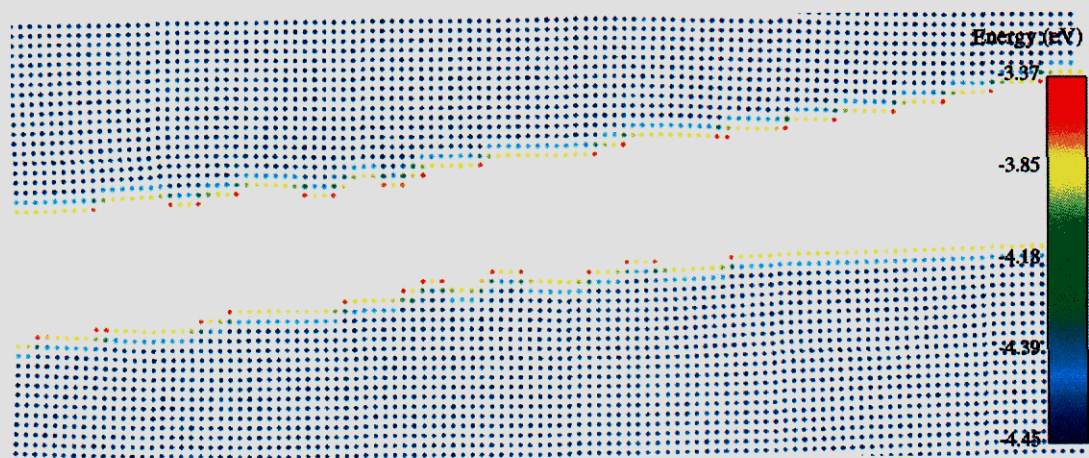
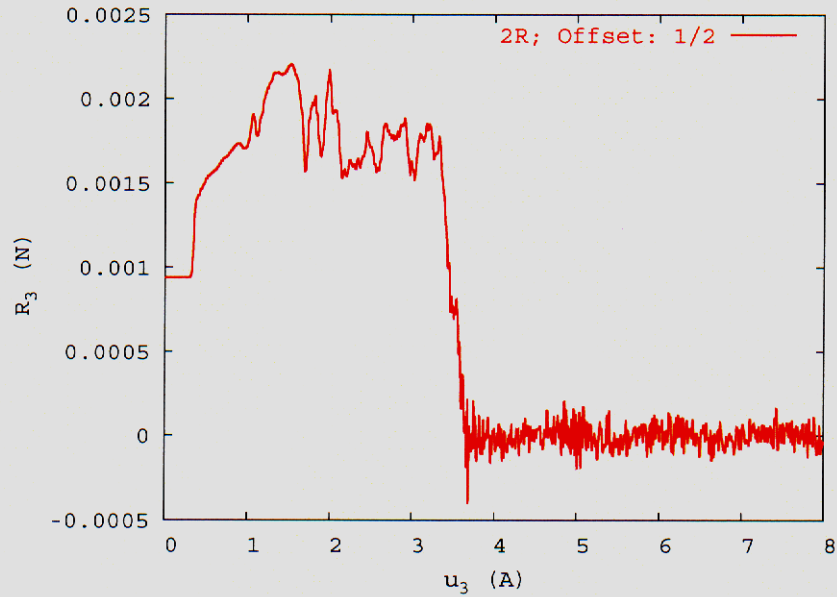
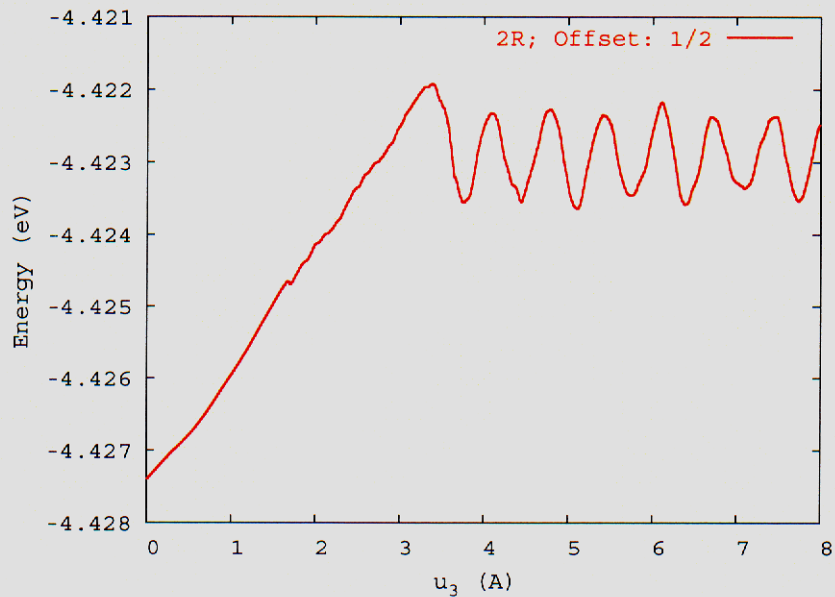


Figure 4.11: Close-up of the final state of the atoms after molecular dynamics simulation for a physical dimension problem after separation



(a) Displacement vs. Reaction force of the top asperity on the bottom one for a rate of 7 Angstroms per millisecond.



(b) Displacement vs. total energy for a rate of 7 Angstroms/millisecond.

Figure 4.12: Reaction force on top and Energy per atom on the bottom for an offset of $1/2$ for a physical dimension problem

Chapter 5

Conclusion

The method described in this report permits the study of local minima of a system as well as an estimate of the force necessary to separate the gears while a nano-scale junction has appeared. It gives an indication of highly probable configurations of the system which can correspond to the system's state after dormancy or to most preferred states of the system at equilibrium if the system in consideration is isolated thermally.

The results show that two asperities in pure nickel tend to bond and a certain amount of force is required to separate them when the system they form is activated again. This force is equal to the force necessary to break the bonds of nickel or to reestablish the position of atoms which have been stretched away from their initial positions. We have shown that the use of atomistic techniques provides an estimate of the reaction force or similarly of the adhesion force exerted from one asperity to the other. Bonding of the two surfaces almost in contact is the only phenomena observed in these simulations during the minimization step, we did not observe any atom diffusion from the bulk or from the surface located outside the interface.

Furthermore, in the simplified case of a perfect lattice considered here, the energy minimum associated with this system correspond to the minimization of the energy at the interface between asperities. The atoms in the bulk are just compressed towards the interface. The system tends to return to the closest perfect lattice corresponding to the initial configuration it was given to. The solution found is only a local minimum of the system because we used conjugate gradient methods. It does not correspond to the best possible minimum of the system.

We have varied two parameters, the radius and the offset. These tests cases have permitted us to show that atoms that are really reacting are the one which are close enough to be within the cut-off region. This is particularly visible at the interface between two asperities. If the two asperities are too distant from each other nothing happens.

This page intentionally left blank.

Chapter 6

Future Work

The preliminary results shown in this report are a first step towards the determination of the evolution of the interface of two gears in contact over a long period of time. We have shown that the minimization techniques give plausible solutions to the problem but they are far from being complete, and also far from real applications. These results lead to two directions of research.

1. The first direction of research is to devise the preferred configurations of the system, the most important one is the global energy minimum, for it has the highest probability of being the configuration after dormancy.
2. The second one is to add more physics to the problem. A real system of gears in contact have many defects and residues. Defects come from the materials, and residues can have many different sources such as the manufacturing process or external parameters.

The idea we want to develop for the first direction of research is the following: it is based on the theory of conformational analysis [Leach, 2000]. It consists of studying the conformations of the system and their influence on its properties. A key component of the conformational analysis is the conformational search, the objective of which is to identify the preferred conformations of a metal. This requires us to locate conformations that are at minimum points on the surface. The main feature of energy minimization algorithms is that they move to the minimum point that is closest to the starting structure. For this reason it is fundamental to have a separate algorithm which generates initial structure for subsequent minimization. An important difference between a conformational search and molecular dynamics or Monte Carlo simulation is that the conformational search is concerned solely with locating minimum energy structures whereas MD or MC generates an ensemble of states that includes structures not at energy minima.

There can be many minima on the energy surface and it is then impractical to try to find them all. Under such circumstances it is often assumed that the naturally occurring conformation is the one with the very lowest value of the energy function. This conformation is usually referred to as the global minimum energy conformation.

Many conformational search algorithms exist in the literature (for a review, see [Leach, 2000]). We plan to implement the random search algorithm because it is the one that fits best with the

CHAPTER 6. FUTURE WORK

problem we want to solve. This approach allows the search of a global energy minimum and not only a local one.

The algorithm consists of doing a random change to the current configuration at each iteration. The new structure is then refined using energy minimization. If the minimized conformation has not been found yet it is stored. The conformation to be used as the starting point for the next iteration is then chosen and the cycle starts again. The procedure continues until a given number of iterations have been performed or until it is decided that no new conformations can be found.

The main issue is then to find the best way to perform these random moves. This is where random smart moves have to be defined. They are called smart because they are specifically efficient for this particular problem. We have noticed that in the system constituted of two asperities in contact, the interface in contact is the more likely to be modified during aging. The atoms in the bulk being more stable, we chose to move more often atoms located at the surface and at the interface than the ones located in the bulk. Two Monte Carlo moves permit us to reach this goal: biased Monte Carlo and cluster moves. We believe that a combination of these moves will be very efficient in finding quickly the global minimum of the system and will permit us to determine the preferred conformational state of the system.

The second direction we plan to investigate is the study of possible contaminants of the surface which can prevent the system to work again after aging. We are specially interested in the effect of oxygen at the interface of the asperities. Nickel does not interact much with oxygen and only a small number of layers will be modified by the presence of atoms of oxygen. This feature is essential in determining the shape and surface energy of the interface between two asperities. A molecular dynamics study of the evolution with time of the penetration of the oxygen atoms from the surface to the bulk can be done. We think that even for the short period of time reached by MD simulations, a trend of the rate of penetration can be deduced and extrapolated to longer time.

Bibliography

- [Baskes, 1997] Baskes, M. I. (1997). Determination of modified embedded atom method parameters for nickel. *Materials Chemistry and Physics*, 50:152–158.
- [Brück et al., 2000] Brück, R., Rizvi, N., and Schmidt, A. (2000). *Applied Microtechnology LIGA-Laser-Micro Precision Engineering*. Hanser.
- [Chandross et al., 2003] Chandross, M., Grest, G. S., and Stevens, M. J. (2003). Friction between alkylsilane monolayers: Molecular simulation of ordered monolayers. Sand Report SAND2002-0540J.
- [Daw, 1989] Daw, M. (1989). Model of metallic cohesion: The embedded-atom method. *Phys. Rev. B*, 39:7441–52.
- [Daw and Baskes, 1983] Daw, M. and Baskes, M. (1983). Semiempirical quantum mechanical calculation of hydrogen embrittlement in metals. *Physical Review Letters*, 50(17):1285 – 8.
- [Daw and Baskes, 1984] Daw, M. S. and Baskes, M. I. (1984). Embedded-atom method: Derivation and application to impurities, surfaces, and other defects in metals. *Phys. Rev. B*, 29(12):6443–6453.
- [DeBoer and Mayer, 2001] DeBoer, M. and Mayer, T. M. (2001). Tribology of mems. *MRS Bulletin*, 26(4):302–04.
- [DeBoer et al., 1999] DeBoer, M. P., Knapp, J. A., Mayer, T. M., and Michalske, T. A. (1999). Role of interfacial properties on mems performance and reliability. *Proceedings of the SPIE - The International Society for Optical Engineering*, 3825:2 – 15.
- [DeBoer et al., 2000] DeBoer, M. P., Knapp, J. A., Michalske, T. A., Srinivasan, U., and Maboudian, R. (2000). Adhesion hysteresis of silane coated microcantilevers. *Acta Materialia*, 48(18-19):4531 – 4541.
- [Dugger, 2002] Dugger, M. T. (2002). The science of dormancy: Assuring microsystem reliability. Seminar, June 2002.
- [Foiles et al., 1986] Foiles, S., Baskes, M., and Daw, M. (1986). Embedded-atom-method functions for the FCC metals Cu, Ag, Au, Ni, Pd, Pt, and their alloys. *Phys. Rev. B*, 33:7983–7991.

BIBLIOGRAPHY

- [Frenkel and Smit, 2002] Frenkel, D. and Smit, B. (2002). *Understanding Molecular Simulation. From Algorithms to Applications*. Academic Press.
- [Gear, 1971] Gear, C. (1971). *Numerical Initial Value Problems in Ordinary Differential Equations*. Prentice-Hall, Englewood Cliffs, New Jersey.
- [Greenwood and Williamson, 1966] Greenwood, J. A. and Williamson, J. B. P. (1966). Contact of nominally flat surfaces. *Proceedings Royal Society*, A295(300):[411,412,413].
- [Haile, 1992] Haile, J. (1992). *Molecular Dynamics Simulation Elementary Methods*. John Wiley & Sons, Inc., New York.
- [Hamilton, 2001] Hamilton, J. C. (2001). Grain boundary and aging simulations for microparts. Seminar, Sept. 2001.
- [Leach, 2000] Leach, A. R. (2000). *Molecular modelling : principles and applications*. Harlow, England ; New York : Prentice Hall, 2001.
- [Lemaitre and Chaboche, 1990] Lemaitre, J. and Chaboche, J. L. (1990). *Title Mechanics of solid materials*. Cambridge University Press.
- [LIGA, 2001] LIGA (2001). LIGA technology. "<http://www.ca.sandia.gov/liga/tech.html>".
- [Persson, 2000] Persson, B. N. J. (2000). *Sliding Friction: Physical Principles And Applications*. Springer-Verlag New York Inc.
- [Plimpton, 1995] Plimpton, S. J. (1995). Fast parallel algorithms for short-range molecular dynamics. *J. Comp Phys*, 117:1–19.
- [Prasad et al., 2000] Prasad, S. V., Hall, A. C., and Dugger, M. T. (2000). Characterization of sidewall and planar surfaces of electroformed LIGA parts. Technical report, Sandia Report SAND2000-1702.
- [Press, 1989] Press, W. (1989). *Numerical Recipes: the art of scientific computing*. Cambridge University Press, New York.
- [Redmond et al., 2001] Redmond, J., Reedy, D., Heinstein, M., de Boer, M., Knapp, J., Piekos, E., Wong, C., and Holm, L. (2001). Microscale modeling and simulations. Technical report, Sandia Report SAND2001-3675.
- [Scully, 1975] Scully, J. C. (1975). *Fundamentals of corrosion*. Pergamon.
- [Shewchuk, 1994] Shewchuk, J. (1994). An introduction to the conjugate gradient method without the agonizing pain.

- [Tanner et al., 2000] Tanner, D. M., Smith, N. F., Irwin, L. W., Eaton, W. P., Helgesen, K. S., Clement, J. J., Miller, W. M., Walraven, J. A., Peterson, K. A., Tangyonyong, P., Dugger, M. T., and Miller, S. L. (2000). Mems reliability: Infrastructure, test structures, experiments, and failure modes. Technical report, Sandia Report.
- [Vanderplaats, 1984] Vanderplaats, G. (1984). *Numerical Optimization Techniques for Engineering Design*. McGraw-Hill, Inc., New York.
- [Wright et al., 1995] Wright, L. G., Sethi, V. K., and Markworth, A. K. (1995). A generalized description of the simultaneous processes of scale growth by high-temperature oxidation and removal by erosive impact. *Wear*, 186-187:230–237.
- [Yagi-Watanabe et al., 2001] Yagi-Watanabe, K., Ikeda, Y., Ishii, Y., Inokuchi, T., and Fukutani, H. (2001). Reaction kinetics and mechanism of oxygen adsorption on the ni(110) surface. *Surface Science*, 482-485:122–133.
- [Yang and Kelly, 2002] Yang, N. and Kelly, J. J. (July 2002). Effect of substrate configuration on the grain structure and morphology of electrodeposited Ni for prototyping LIGA. Sandia Report SAND2002-8311.

7.1 DISTRIBUTION:

1	MS 0316	J.B. Aidun, 9235
1		S.J. Plimpton, 9212
1		A. Slepoy, 9235
1		M.J. Stevens, 9235
1		A.P. Thompson, 9235
1	MS 0516	R.G. Spulak, 2564
1	MS 0521	F.M. Bacon, 2502
1	MS 0824	A.C. Ratzel, 9110
1	MS 0841	T.C. Bickel, 9100
1	MS 0847	H.S. Morgan, 9120
1	MS 0871	L.C. Beavis, 14405
1	MS 0885	G.S. Heffelfinger, 1802
1	MS 0886	P.G. Kotula, 1822
1	MS 0889	M.T. Dugger, 01851
1		S.V. Prasad, 01851
1	MS 0893	J.V. Cox, 8725
1		E.D. Reedy Jr., 9123
1	MS 1411	H.E. Fang, 1834
1		C.C. Battaile, 1834
1		M.V. Braginsky, 1834
1		S.M. Foiles, 1834
1		E.A. Holm, 1834
1		J.J. Hoyt, 1834
1		E.B. Webb III, 1834
1	MS 1415	J.E. Houston, 1114
1	MS 1427	J.M. Phillips, 1100

7.1. DISTRIBUTION

1	MS 9001	M.E. John, 8000 Attn: J. Vitko, 8100, MS 9004 D.R. Henson, 8200, MS 9007 W.J. McLean, 8300, MS 9054 P.N. Smith, 8500, MS 9002 K.E. Washington, 8900, MS 9003
1	MS 9042	P.A. Spence, 8727
1		P.M. Gullett, 8727
1	MS 9052	S.F. Rice, 8361
1	MS 9108	R.D. Monson, 8243
1		C.A. Lajeunesse, 8243
1		C.W. Pretzel, 8243
1		S.L. Robinson, 8243
1		G.C. Story, 8243
1	MS 9161	E.P. Chen, 8726
1		C.J. Kimmer, 8726
1		P.A. Klein, 8726
1		D.A. Zeigler, 8726
10		J.A. Zimmerman, 8726
1	MS 9161	J.C. Hamilton, 8721
1		D. Medlin, 8721
1		D.J. Siegal, 8721
1	MS 9202	R.M. Zurn, 8205
1	MS 9402	C.H. Cadden, 8724
1		R. Causey, 8724
1		D.F. Cowgill, 8724
1		K.L. Hertz, 8724
1		B.P. Somerday, 8724
1	MS 9403	J.C.F. Wang, 8723
1		A.J. Antolak, 8723
1		E.H. Majzoub, 8723
1		D.H. Morse, 8723
1		N. Yang, 8723

BIBLIOGRAPHY

- 1 MS 9404 S.H. Goods, 8725
1 S. Lee, 8725
- 1 MS 9405 R.H. Stulen, 8700
Attn:
G.D. Kubiak, 8705, MS 9409
R.Q. Hwang, 8721, MS 9161
W.R. Even Jr., 8722, MS 9403
J.R. Garcia, 8725, MS 9042
C.C. Henderson, 8729, MS 9401
J.E.M. Goldsmith, 8730, MS 9409
W.C. Replogle, 8731, MS 9409
- 1 MS 9405 K.L. Wilson, 8703
- 15 MS 9405 S. Aubry, 8726
1 D.J. Bammann, 8726
1 A.A. Brown, 8726
1 G.R. Feijoo, 8726
1 J.W. Foulk, 8726
1 Y. Hammi, 8726
1 D.A. Hughes, 8726
5 R.E. Jones, 8726
1 E.B. Marin, 8726
1 R.A. Regueiro, 8726
- 1 MS 9950 T.D. Nguyen, 8726
1 MS 9950 G.J. Wagner, 8728
- 1 LANL B.A. Meyer, ESA-GTS, C934
1 K.G. Honnell, ESA-GTS, C934
- 1 LLNL W.G. Wolfer, L353
1 C.R. Krenn, L353
1 K.A. Winer, L170
1 S. Sack, L170
- 3 MS 9018 Central Technical Files, 8945-1
1 MS 0899 Technical Library, 9616
1 MS 9021 Classification Office, 8511/
Technical Library, MS 0899, 9616
1 DOE/OSTI via URL